Room Acoustic Measurements under the Influence of Flight Noise from Quadcopter UAVs

Eric Kurz

Signal Processing and Speech Communication Laboratory (SPSC), Graz University of Technology, 8010 Graz, Austria

Email: eric.kurz@tugraz.at

Introduction

Although the ISO 3382-1 standard mentions inhomogeneities of the sound field, a comparatively low spatial density of receiver positions is proposed for measurement [1]. Furthermore, room acoustic measures are partly subject to strong location-dependent fluctuations, as De Vries et al. have shown in studies in 2001 [2]. Therefore, room acoustic measurements with high spatial resolution, which cause a high technical or temporal effort, are necessary. On the one hand, measurements carried out manually by Akama et al. in 2010 were technically not very complex, but very time-consuming [3]. On the other hand, automated measurements with a large-area microphone array, as carried out by Witew et al., can considerably reduce the measurement time but come with high technical effort [4]. In any case, the sound field can be examined very precisely with both methods. Another possibility to scan sound fields with high resolution is offered by robots, which usually move on the ground [5] or in the air. An interesting approach for a measuring robot based on a miniature airship comes from a Polish research group [6, 7]. With this technique, it is possible to scan arbitrary receiver position in a spatial volume silently while the miniature airship hovers stationary. One disadvantage of this technique is the distortion of the sound field by the airship itself.

Nowadays, the use of quadcopter unmanned aerial vehicles (UAVs) is becoming increasingly popular in a wide range of civil applications. Another promising application for these UAVs would be to perform automated room acoustic measurements with high spatial resolution. When carrying out room acoustic measurements, the UAV's free movement in space allows to measure over non flat surfaces or areas with obstacles (e.g. fixed seating). Also stable hovering flight is possible with today's quadcopter UAVs. However, this technology brings some disadvantages. The UAV must be located and positioned throughout the measurement period. Due to the permanent positioning process, slight movements are possible during the measurement. A major disadvantage is the noise radiation during hovering at a fixed position in space as well as possible sound field distortions due to turbulent airflow through the UAV's propellers. Both effects have a considerable influence on the quality of a room acoustic measurement.

This contribution presents a feasibility study regarding the determination of the reverberation time by room impulse response (RIR) measurements under the influence of flight noise from a quadcopter UAV. Furthermore, influence of the flight noise from the UAV on the quality of the reverberation time estimation is investigated. For this purpose, spectral and directional flight noise radiation characteristics of the UAV and an optimal mounting position of the measurement microphone/s on the UAV are determined. Subsequently, room acoustic measurements are performed with and without present flight noise from the UAV. The recorded RIRs are used to evaluate the quality of reverberation time estimation in dependence on the noise radiated by the UAV. Finally, noise compensation methods (NCMs) are examined and compared by means of reverberation time estimation.

Noise radiation of UAVs

First, the noise radiation of the UAV has to be characterised spectrally and directionally. Therefore, a measurement of the sound radiation of a DJI Mavic 2 quadcopter UAV was carried out in the recording studio of the SPSC laboratory. The sound radiation pattern of the UAV was measured during a propeller speed run-up using a semi-circular microphone array consisting of 13 equally spaced measurement microphones at a radius of $r = 1$ m (cf. fig. 1). After each run-up, the UAV was rotated in azimuth φ by 15°. With this procedure, a radiation pattern resolution of 15° in azimuth φ and zenith ϑ with 266 measurement points was generated. The recorded time signals were processed using a short-time Fourier transform (STFT) and a spherical harmonic decomposition of order $n = 7$ according to [8].

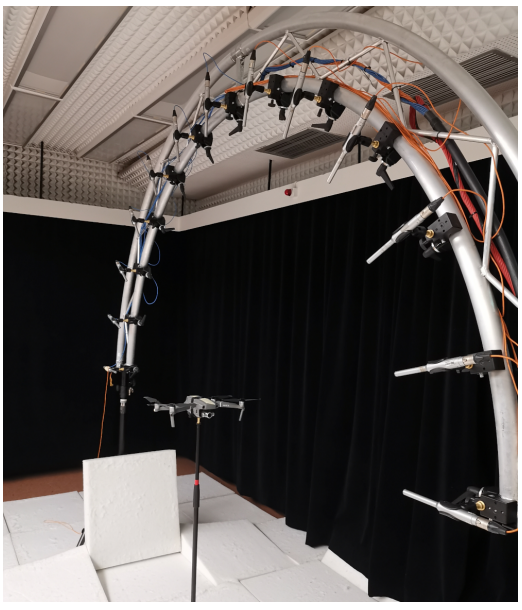

Figure 1: Measurement setup for determining the UAV's radiation patterns.

Fig. 2 shows the spectrogram of the noise radiation in the horizontal plane directly in front of the UAV during the propeller speed run-up. It can be seen that the radiated noise spectrum consists of broadband noise and discrete harmonic components. The sound pressure level (SPL) of the broadband noise as well as the harmonic components increases with increasing rotational speed of the propellers. Also, the frequency of the harmonic components raise proportionally.

The directional characteristics of the noise radiation of the UAV for the propeller rotational speed of 4900 RPM (hovering state) are depicted in balloon plots (fig. 3) in octave bands from 125 Hz to 8 kHz. There are significant noise contributions in horizontal planes with constant zenith angle, especially in the upper hemisphere. Additionally, there is strong noise radiation at the poles of the radiation patterns. The noise radiation at the nadir of the radiation patterns is caused by the air flow of the propellers and consists mainlyof low frequency components. In general, the biggest contributions to the noise sound pressure level are generated in a frequency range from 125 Hz to 1 kHz. Based on these findings, it is reasonable to mount one or more measurement microphones in the lower hemisphere of the UAV ($\vartheta \approx 120°$) in order to pick up as little flight noise as possible.

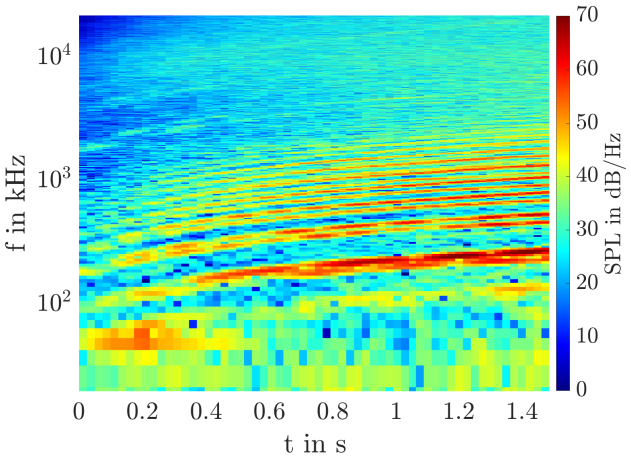

Figure 2: Spectrogram of the flight noise from the UAV for a propeller speed run-up.

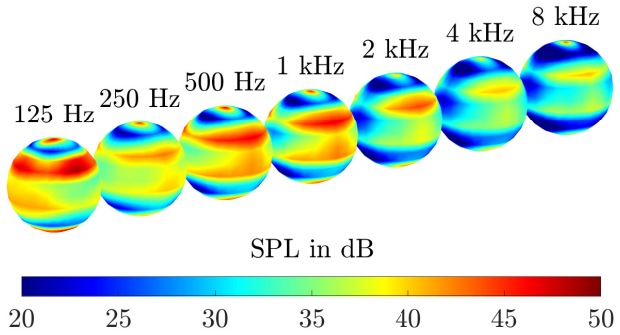

Figure 3: Radiation patterns of the flight noise from the UAV for a propeller rotation speed of 4900 RPM in octave bands from 125 Hz to 8 kHz.

Noise compensation methods

For our investigations a simple additive noise model is assumed, i.e. with some simplifications one can say that the recorded impulse response $\hat{p}(t)$ is composed of the RIR $p_{\mathrm{RIR}}(t)$, which can be obtained from the excitation of the room with a corresponding source signal, and the flight noise of the UAV $n(t)$ (1).

$$\hat{p}(t) = p_{\mathrm{RIR}}(t) + n(t) \tag{1}$$

The Energy Decay Curve (EDC) $E(t)$ is obtained from the RIR by means of squaring and subsequent backward integration (2). Consequently, the additive interference signal directly affects the determination of the EDC.

$$E(t) = \int_t^{t_{\mathrm{RIR}}} \hat{p}^2(\tau) d\tau \tag{2}$$

In the 2014 paper by Guski and Vorländer, noise compensation methods (NCMs) for the signal model in eq. (1) are discussed [9]. In this paper, however, an uncorrelated additive white Gaussian noise is assumed for $n(t)$. The NCMs are used to estimate the EDC, and subsequently the reverberation time, from noisy RIR as robustly as possible.

Truncation at intersection time t_i

First, one can try to find the intersection of the signal energy decay and the noise iteratively with the Lundeby algorithm [10] and cut off the EDC directly at t_i (3). This method is part of ISO 3382-1 [1].

$$E(t) = \int_t^{t_i} \hat{p}^2(\tau) d\tau \tag{3}$$

Truncation and correction

In a second step, the truncated part of the EDC can be compensated with the ernergetic term C_{comp} gained by a linear regression according to [10] (4). This method is also mentioned in the ISO 3382-1 standard [1].

$$E(t) = \int_t^{t_i} \hat{p}^2(\tau) d\tau + C_{\mathrm{comp}} \tag{4}$$

Noise subtraction

Another possibility is to subtract the noise from the squared impulse response before the backward integration as proposed by Chu in 1978 [11].

$$E(t) = \int_t^{t_{\mathrm{RIR}}} (\hat{p}^2(\tau) - \overline{n}^2) d\tau \tag{5}$$

Noise subtraction, truncation and correction

The last method combines all the for mentioned techniques (cf. (6) with (3) to (5)).

$$E(t) = \int_t^{t_i} (\hat{p}^2(\tau) - \overline{n}^2) d\tau + C_{\mathrm{comp}} \tag{6}$$

Measurement

A measurement was carried out in the lecture hall HSi2 at Graz University of Technology according to ISO 3382-1 [1]. The lecture hall was chosen since its acoustic properties are well documented from previous investigations

[12]. It has a footprint of 15.5 m by 10.5 m and an average height of 3.5 m resulting in a volume of approx. 576 m^3. Four measurements with 5 repetitions each with fixed omnidirectional sound source and measurement microphone positions were performed (cf. fig. 4). The omnidirectional sound source played back an exponential sine sweep with a duration of approx. 3 s (FFT degree $N = 17$) and a sound pressure level of approx. 100 dB. To generate the ground truth, a reference measurement was carried out without flight noise from the UAV. For the other measurements, the UAV was flown to positions UAVP1 to UAVP3 relative to the measurement microphone as shown in fig. 5.

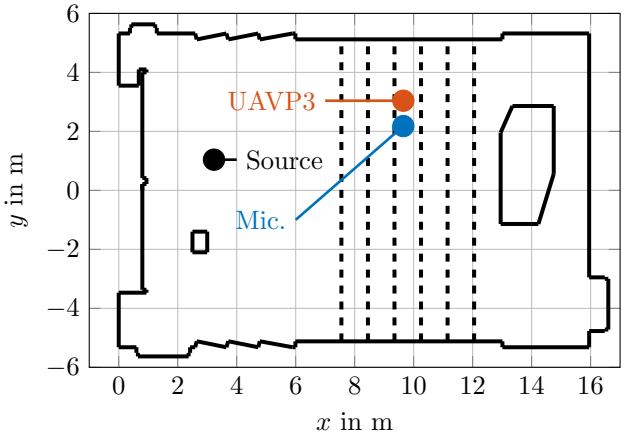

Figure 4: Floorplan of the lecture hall HSi2 with fixed sound source and measurement microphone positions as well as the position of the UAV (UAVP3).

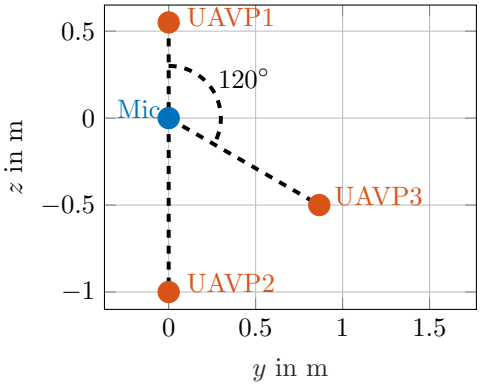

Figure 5: Relative positions UAVP1 to UAVP3 of the UAV to the measurement microphone.

Results

The determined reference reverberation time $T_{20} = 0.93$ s corresponds well with results of previous investigations [12]. There are also no inconsistencies in the EDCs of the reference measurement (cf. solid lines in fig. 6). Using the determined reverberation time and the room volume, a Schröder frequency of $f_S = 80$ Hz can be calculated. Consequently, an analysis is carried out in the octave bands from 125 Hz to 8 kHz in order to exclude the influence of pronounced single modes.

Table 1 shows the relative deviations of the estimation of T_{20} for UAVP1 to UAVP3 from the reference measurement. First of all, one can see the strong overestimation of the reverberation time of the measurement at UAVP1, except in the 4 kHz octave band. This is caused by the very low peak-signal-to-noise ratio (PSNR) for this UAV position, which is also clearly visible in the resulting EDCs (cf. fig. 6, dashed lines). For position UAVP2, the higher PSNR leads to a fair result for T_{20} even without any NCM, except from the 8 kHz octave band. Significant overestimation happens in the 1 and 2 kHz octave bands, where the PSNR is below the critical value of ≈ 60 dB. Even better T_{20} estimation can be achieved with UAVP3, again except in the 8 kHz octave band although a fair PSNR ≈ 60 dB is reached. All results are in good accordance with the investigations from [9]. To further improve the reverberation time estimation results, the NCMs are applied to the UAVP3 data and their performance is compared.

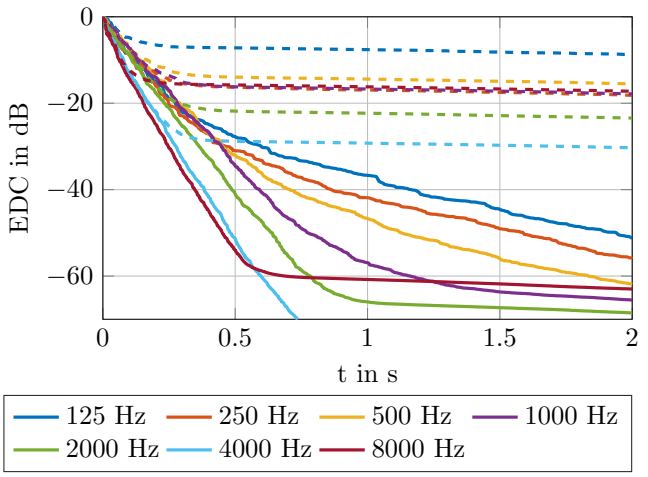

Figure 6: EDCs of reference (solid line) and UAVP1 (dashed) measurement in octave bands from 125 Hz to 8 kHz.

Table 1: Relative deviations ΔT_{20} from the reference measurement and PSNR for UAVP1 to UAVP3 in octave bands.

f in Hz	UAVP1		UAVP2		UAVP3	
	ΔT_{20} in %	PSNR in dB	ΔT_{20} in %	PSNR in dB	ΔT_{20} in %	PSNR in dB
125	2533	30.0	4.6	63.4	5.0	61.2
250	3439	43.2	2.2	62.2	-2.4	65.7
500	3393	41.2	2.1	59.2	0.6	60.8
1000	3505	45.4	14.5	56.5	4.1	59.3
2000	3352	52.4	23.3	57.2	4.3	60.5
4000	7.5	64.1	3.5	67.0	0.1	71.3
8000	6530	50.9	6485	53.4	6397	59.7

Performance Comparison of NCM

As an example, the EDCs for UAVP3 with NCMs applied as well as the untreated EDC and the reference EDC for the 2 kHz octave band are plotted in Fig. 7. It is clearly evident that all NCMs can increase the available dynamic range of the EDC by approx. 20 dB. However, there is a slight underestimation of the reference EDC by all NCMs.

In order to examine these underestimations in more detail, the relative deviations of the early decay time (EDT) ΔEDT and the reverberation times ΔT_{20} and ΔT_{30} from those of the reference measurement are calculated for each octave band. Median values of ΔEDT, ΔT_{20} and ΔT_{30} with corresponding 95% confidence intervals, interquartile ranges (IQR), whiskers and outliers were cal-

culated for each NCM and are plotted as boxplots in fig. 8. First, it is noticeable that all NCMs tend to underestimate the corresponding reverberation time. Interestingly, the EDT, which requires a small dynamic range, is underestimated the most. This behaviour cannot be seen in fig. 8. Due to the small dynamic range required for the calculation of the EDT, the performance of the NCMs is identical. However, this behaviour changes if a larger dynamic range is required for the calculation of the corresponding reverberation time or if calculation would not even be possible without noise compensation, respectively. The NCMs that use truncation perform better in estimating T_{30}, albeit not significantly. Best and most robust estimation of T_{30} is done with the NCM "Truncation and Correction" with maximum deviation of $\Delta T_{30} \approx -3\%$ and no outliers in individual octave bands.

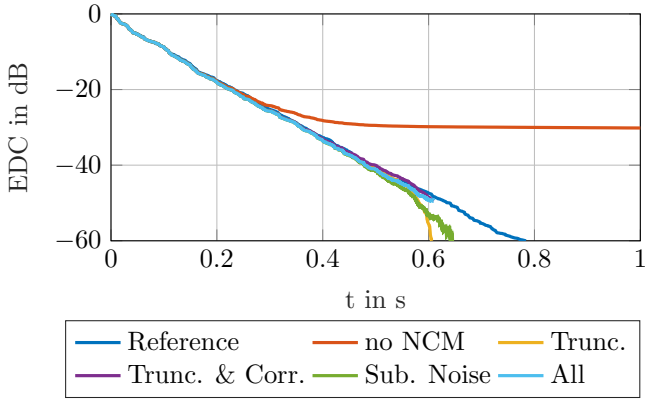

Figure 7: EDC of reference and UAVP3 measurement (with and without NCMs) for the 2 kHz octave band.

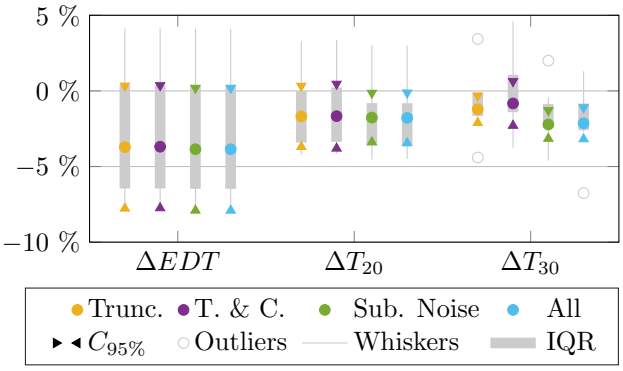

Figure 8: Boxplots with median values (•) of the relative deviations ΔEDT, ΔT_{20} and ΔT_{30} for UAVP3.

Conclusion

In this paper, a feasibility study was conducted on the use of a UAV as a probe carrier for measuring reverberation times, despite its high levels of radiated noise. For this purpose, it was shown that significant portions of the noise are radiated in the vertical directions and in the upper hemisphere of the UAV. Consequently, one or more measurement microphones should be mounted in the lower hemisphere of the UAV, but not directly in the airflow of the propellers ($\vartheta \approx 120°$). Furthermore, it was shown that the noise of the UAV has a critical influence on the accuracy of the reverberation time estimation. If the PSNR falls below a critical value, a valid estimation of the reverberation time is no longer possible. To address this issue, NCMs were used in the calculation of EDCs and their influence on the accuracy of reverberation time estimation was investigated. Results of this investigation are in good accordance with [9]. It was shown that the NCM "Truncation and Correction" (optional in the ISO 3382-1 standard [1]) provides best results for reverberation time estimation with an deviation of less than −3%. Based on the results in this paper, it can be concluded that a reverberation time measurement according to ISO 3382-1 standard is feasible with an UAV.

References

[1] EN ISO 3382-1: Acoustics – Measurement of room parameters – Part 1: Performance spaces. International Organization for Standardization (2009)

[2] de Vries, D. et al.: Spatial fluctuations in measures for spaciousness. Journal of the Acoustical Society of America (2001), vol. 110, no. 2, 947-954

[3] Akama, T. et al.: Distribution of selected monaural acoustical parameters in concert halls. Applied Acoustics (2010), vol. 71, 564-577

[4] Witew, I. B. et al.: Sampling the sound field in auditoria using large natural scale array measurements. The Journal of the Acoustical Society of America (2017), vol. 141, no. 3

[5] Uehara, M. et al.: Visualization of Distribution of Room Acoustic Parameters by Using Mobile Robot. Proceedings of the 23rd International Congress on Acoustics (2019)

[6] Majkut, L. et al.: Acoustic Field Distortions Caused by Helium Filled Balloons. Acta Physica Polonica A (2014), vol. 125, no. 4 A, 84-87

[7] Borkowski, B. and Pluta, M.: Automated Measurement System for Room Acoustics an Initial Feasibility Study. Archives of Acoustics (2015), vol. 40, no. 3, 419-428

[8] Ahrens, J. and Bilbao, S.: Computation of Spherical Harmonics Based Sound Source Directivity Models from Sparse Measurement Data. Forum Acusticum (2020)

[9] Guski, M. and Vorländer, M.: Comparison of Noise Compensation Methods for Room Acoustic Impulse Response Evaluations. Acta Acustica united with Acustica (2014), vol. 100, 320-327

[10] Lundeby, A. et al.: Uncertainties of Measurements in Room Acoustics. Acustica (1995), vol. 81, 344-355

[11] Chu, W. T.: Comparison of reverberation measurements using Schroeder's impulse method and decay curve averaging method. Acoustical Society of America (1978), vol. 63, 1444-1450

[12] Frischmann, C. et al.: Akustische Bestandsaufnahme der TU-Hörsäle Inffeldgasse. Bachelor's Thesis, TU Graz (2018)

[13] Berzborn, M. et al.: The ITA Toolbox: An Open Source MATLAB Toolbox for Acoustic Measurements and Signal Processing. DAGA Proceedings (2017), 222-225